Characterizing Northwest weather patterns for prescribed burning and smoke management

Andy Chiodi (chiodi@uw.edu)

1. Background.

Large wildfires, whether initiated by human actions or the result of entirely natural actions, often have very potent consequences for the communities that are affected by them or are at risk of being affected. In 2017, the direct cost of wildland fire suppression efforts incurred by the U.S. Forest Service exceeded $2 billion USD for the first time in history. In addition to the additional direct financial costs associated with property damage, the indirect costs via air quality harm on residents and damage to infrastructure including water and soil quality, are also considerable. Due to emissions from historically large wildfires, breathable air quality in the Pacific Northwest gained national attention for being, over much of a week in the latter half of the 2017 fire season, worse than observed anywhere else in the world. In 2018, smoke from wildfires again contributed multi-day episodes of unhealthy to very unhealthy air quality over much of Washington and Oregon, and Oregon wildfire costs hit a new high of $514 million USD.

The recent extremely large wildfire seasons in the Pacific Northwest in 2015, 2017 and 2018, have motivated discussion between the States of Washington and Oregon and interested agencies including the US Forest Service of how to best deal with the threats of unusually large wildfires. These threats are widely believed to have been exacerbated by management efforts during much of the 20st century that effectively excluded fire from inland Northwest forest and range ecosystems, thereby (unintentionally) causing a buildup of hazardous levels of fuels (Martin and Dell, 1978) as well as an increase in fire susceptible ecosystems (e.g. Hall 1976). Although potentially destructive in especially its extreme form, fire remains a necessary and important part of Northwest forest ecosystem restoration and maintenance.

Prescribed burning has emerged as an essential management tool for maintaining healthy fire-adapted forests and reducing hazardous fuel levels. In order for prescribed burns to be both safe and effective they must be applied within a precise window of weather and fuel moisture conditions. These weather parameters are chosen to provide smoke dispersion and fire behavior that is both intense enough to accomplish its objectives and within our ability to control it. A given burn's specific set of weather and fuel parameters is typically referred to as is 'prescription'. The prescription parameters targeting fire intensity often vary depending on objective. For example, both high and low intensity fires are planned as part of the upcoming Signal Peak prescribed burn, which will take place in the Fishlake National Forest of Utah as part of the Fire and Smoke Model Evaluation Experiement (FASMEE; see Prichard et al. 2019) project. Accordingly, the acceptable set of parameters related to fire behavior, such as near surface wind speed, relative humidity, temperature, and dead and live fuel moistures, have a wide range from one Signal Peak burn unit to the next (e.g., relative humidity 8% to >20%, temperature 85 to < 55 degrees Fahrenheit, mid-flame wind speed 15 mph to 0 mph), whereas

the clearing index (discussed below) criteria in place to insure sufficient smoke dispersion remains the same for each burn unit (specifically, clearing index > 500).

Limited availability of the preferred fire weather conditions, especially in regard to their impact on smoke management, have been cited as a primary barrier to reaching the desired levels and timings of prescribed burn activity (Kobziar et al. 2015; Haines et al. 2001). Over the northwest, reduction of visibility caused by smoke from forest and range burning has been cited as a primary public concern, both as a nuisance to those wishing to enjoy the region's scenic vistas and outdoor recreation opportunities and as a potential traffic hazard (Martin and Dell, 1978). The smoke management plan currently in place over Washington prevents prescribed burning for these reasons on summertime weekends. The question of whether criteria such as this can be modified to produce an overall safer and more effective regional approach to prescribed burning is one being taken up in ongoing efforts to revise the present Smoke Management Plan.

Mixing height and transport wind, along with indices calculated based on them (such as the ventilation index or clearing index; see Hardy et al. 2001, Goodrick et al. 2013) are currently the primary variables used to estimate near surface dispersion conditions for smoke management purposes in the US (e.g. Goodrick et al. 2013). Mixing height has been defined as the height above ground to which ground-released pollutants will disperse based on ambient circulation (Seibert et al. 2000; Fearon et al. 2015). Mixing height is commonly calculated based on the air parcel equilibrium approach (Ferguson et al. 2003; Chiodi et al. 2018, 2019). Transport wind is typically calculated as the vertical average of wind speed from the surface to the mixing height, although Washington State prefers to replace transport wind with wind speed at 10m height (B. Potter, pers. comm.; also done due to practical constraints in place at the time by Ferguson et al. 2003) when estimating ventilation. The ventilation index is (traditionally) the mixing height times the transport wind. The ventilation index offers an estimate of the volume of air into which smoke emitted from the ground will disperse based on ambient atmospheric mixing. A normalized ventilation index, called the "clearing index" is used by several western states to gauge smoke dispersion potential. Specifically, the clearing index is the ventilation index expressed in units of ft · kn divided by 100. In some western US states, such as Utah and Montana, a clearing index of 500 is used to signify ample atmospheric dispersion for prescribed burning. A clearing index value of 500 equates to a ventilation index value of ~7840 $m^2 s^{-1}$.

The importance of improving our understanding of historical patterns of ventilation index variability for the sake of smoke management was recognized over 15 years ago by Ferguson et al. (2003; F03). To examine ventilation index, F03 estimated winds based on results from a ~ 5km horizontal resolution hydrostatic flow model of wind speed at 10m height agl and mixing heights based on interpolating results from radiosonde measurements taken at 00:00 and 12:00 UTC (17:00 and 05:00 PDT) over the available (sparse), research-quality radiosonde stations spread across the US (4 such stations are available over Washington and Oregon, near the cities of Spokane, Quillayute, Salem and Medford). In F03, it was assumed that high mixing heights characteristic of the "free atmosphere" occurred when the surface height at an interpolated location (i.e. some distance away from the radiosonde sites) exceeded the mixing height estimated at the observational sites. Thus, wintertime mixing heights over higher elevation terrain were often assumed to be very high in winter. The resulting data set offered a useful first

look at early morning and evening ventilation index behavior across the US. FO3 offered a rating system for poor (0-1175), marginal (1176-2350), fair (2351-3525) and good (>3525 m2 s-1) ventilation potential that used category thresholds one half as large as those suggested by Hardy et al. (2001), in which case ventilation index was calculated as the planetary boundary layer height times 40 m wind speed (Hardy et al. Table 9.1, pg 164). Thus, factors of conversion between mixing height calculated via the parcel equilibrium approach and model generated planetary boundary layer heights, as well as transport wind calculated traditionally, or using fixed height winds (e.g. 10 m) are important to quantify over the Northwest.

Quantifying the relationship between summertime and shoulder season (spring and fall) smoke dispersion conditions would also be potentially quite useful to regional fire managers for the following reasons: The 2019 fire season over Washington and Oregon was relatively tame compared to 2017 and 2018. In 2019, resources (e.g. fire crews) that would have been fully engaged in fire suppression efforts in years like 2017 or 2018 were available for other wildland fire management efforts. Lightning strikes and thus naturally ignited fires are most common in the summer. If some of the naturally ignited fires in years like 2019 were managed for fuel reduction and ecological benefit (as if they were prescribed) then this could greatly expand the number of acres treated over the region without much more added expense. However, an expanded 'social license' would be needed to achieve this, that is, public and other agency support for allowing more natural-ignition fires to burn long enough to garner fuel-reduction and ecological benefits, rather than being suppressed immediately. Smoke impacts and the public's perception of them are key to this situation. Thus, quantifying seasonal differences in the atmosphere's capacity to disperse smoke and thus maintain acceptable breathable air quality during managed fires is critical to the ongoing discussion of how to best manage wildland fire over this region.

Summary of Accomplishments

The funding provided by this grant from the Joint Institute for the Study of the Atmosphere and Ocean has allowed the PI to:

- Collect and process a 10-yr long fire weather data set based on hourly and 4km resolution University of Washington/Northwest Regional Modeling Consortium (Mass et al. 2003) historical numerical weather prediction data (see Data and Methods)
- Calculate the climatology of key smoke dispersion weather variables, including the ventilation index and the variables used to calculate ventilation index, over the Northwest (see Smoke Dispersion Climatology).
- Examine how the assessment of smoke dispersion changes with choice of underlying variable (e.g. using 10-m wind speed rather than transport winds; see Parameter Sensitivity section)
- Examine the drivers of ventilation extremes and how they change with season over the Northwest (see Characterizing Variability section)

2. Data and Methods.

The core surface and atmospheric data used in this analysis comes from archived numerical weather model forecasts issued by the University of Washington. The forecast data examined herein was generated operationally using nested Weather Research and Forecasting (WRF) model runs with an inner 4km horizontal resolution grid that covers all of Washington, Oregon and Idaho, along with the western third of Montana and Wyoming and northernmost parts of California, Nevada and Utah. A map of the 4 km resolution terrain used in the present model configuration is shown in Fig. 1. The archive used in this study dates back to June 2009 and extends through 2018. Daily forecast model runs were initialized at 00:00 Coordinated Universal Time (UTC) and were run for an 84 hour forecast period with output saved hourly. We have time-aggregated the 12:00 UTC through 35:00 UTC hourly forecasts from each day in the 1 June 2009 through 31 December 2018 period to form a continuous hourly record of forecast data over this ~10 yr period. The 12:00 UTC - 35:00 UTC period was selected for optimal forecast skill, excluding the spin-up period (~first 12 hours of forecast) and probable skill degradation at longer leads. Because most burning takes place between 10 am and 2 pm local time, a 'day-time' data set was produced by averaging over those hours.

The physics packages implemented presently in the Pacific Northwest mesoscale forecast model include the Yonsei University planetary boundary layer scheme, with the Noah-MP land surface model and Grell-Freitas cumulous convection. Because forecast skill improvements are constantly sought, changes to the model configuration have been and very likely will continue to be made. For example, the Grell-Freitas cumulus convection scheme replaced the Simplified Arakawa Schubert scheme in November 2015 and The WRF version 3.4.1 unmodified YSU PBL scheme replaced a modified version of the 3.1.1 YSU scheme in October 2012. Also, the inner-nest domain of the operational Pacific Northwest forecasts was expanded by about 10% in the west and north direction in October of 2011. A log of this and other changes made to the model parameterization is available at https://a.atmos.washington.edu/mm5rt/log.html. Pre-October 2011 data have been regridded to the present horizontal grid to facilitate analysis across the domain expansion.

The air parcel equilibrium height method is used to estimate mixing height. Equilibrium height is calculated as the height above ground to which an air parcel heated to the surface temperature would rise (in the case that it is buoyant compared to surrounding air) before it becomes neutrally buoyant at some higher altitude. The equilibrium height method is commonly used by National Weather Service Forecast Offices when issuing mixing height forecasts, and has been found to provide an effective estimate for the mixing height determined over the contiguous US from lidar measurements (Fearon et al. 2015) when virtual potential temperature (which includes the effects of water vapor), rather than potential temperature (which does not include water vapor effects) is used a proxy for air density (c.f. Stull, 1991; Holzworth 1964; 1967).

The core atmospheric variables from WRF needed to calculate mixing height via the equilibrium height approach are geopotential height (for estimating model layer altitudes), vertical profiles of water vapor mixing ratio, potential temperature and pressure, as well as the height (above sea

level) pressure, potential temperature and mixing ratio at the planetary surface. The standard formulae recounted by Stull (1988; pgs 7, 276 and 551) were used to compute vertical profiles of virtual potential temperature at each horizontal grid point, along with the ground surface virtual potential temperature.

Transport wind was calculated as the average wind speed between the planetary surface and the mixing height. When stable near-surface vertical profiles of virtual potential temperature are forecasted by the model, both mixing height and transport wind are assigned the value of zero.

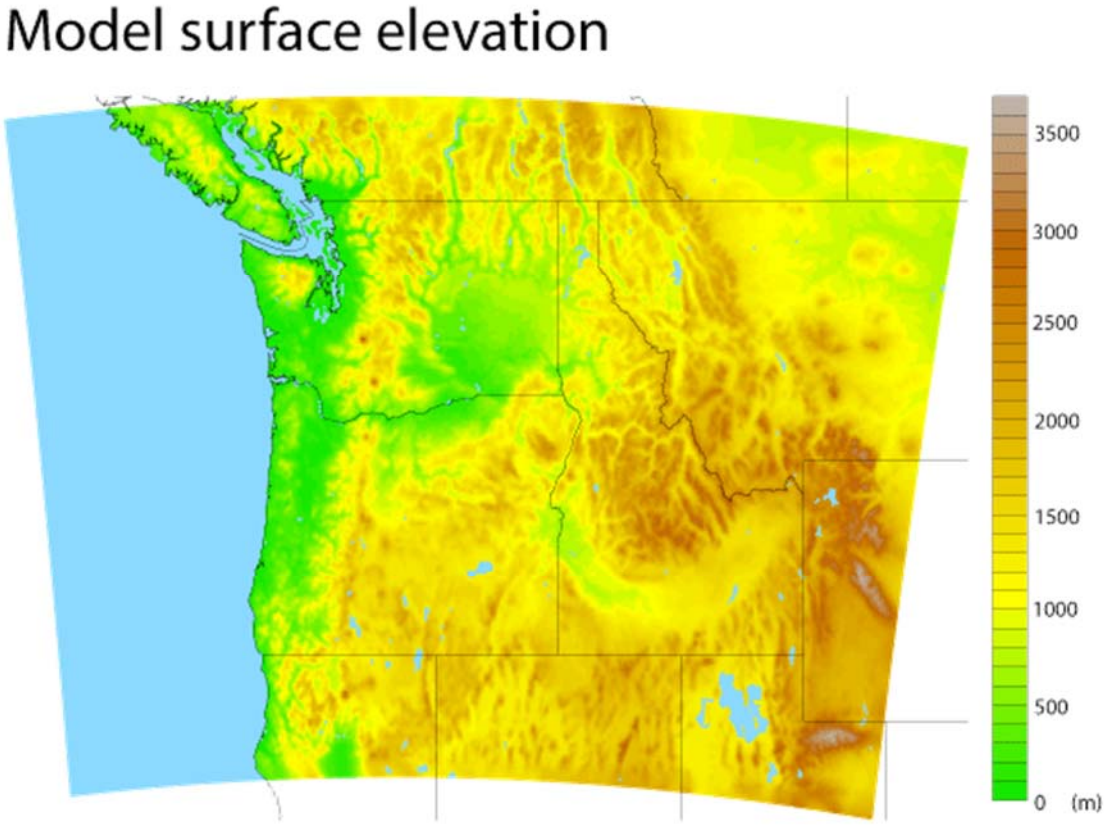

Figure 1. 4km horizontal resolution WRF model surface elevation.

3. Smoke Dispersion Climatology

We begin with documentation of the daytime (10am-2pm local) mixing height, transport wind and ventilation index monthly climatology calculated from the 10-yr WRF data set. Mixing height exhibits minima at all locations in the cold season (November to February) and maxima in the late spring and summer (May through August). Spring/summer maxima are regionally highest in the elevated plateaus of northern Nevada, Utah and Wyoming. Summertime heights remain high (> 3500 m) over southeastern Oregon and, to a lesser extent (> 2500 m), the Washington Columbia Basin region. Western Washington and Oregon and the highest elevations of the Washington and Oregon Cascade Mountains exhibit more limited summertime

maxima than the inland plateaus, with southeastern Oregon mixing height remaining under ~2000m during all months, in the climatological averaged sense (Fig. 2).

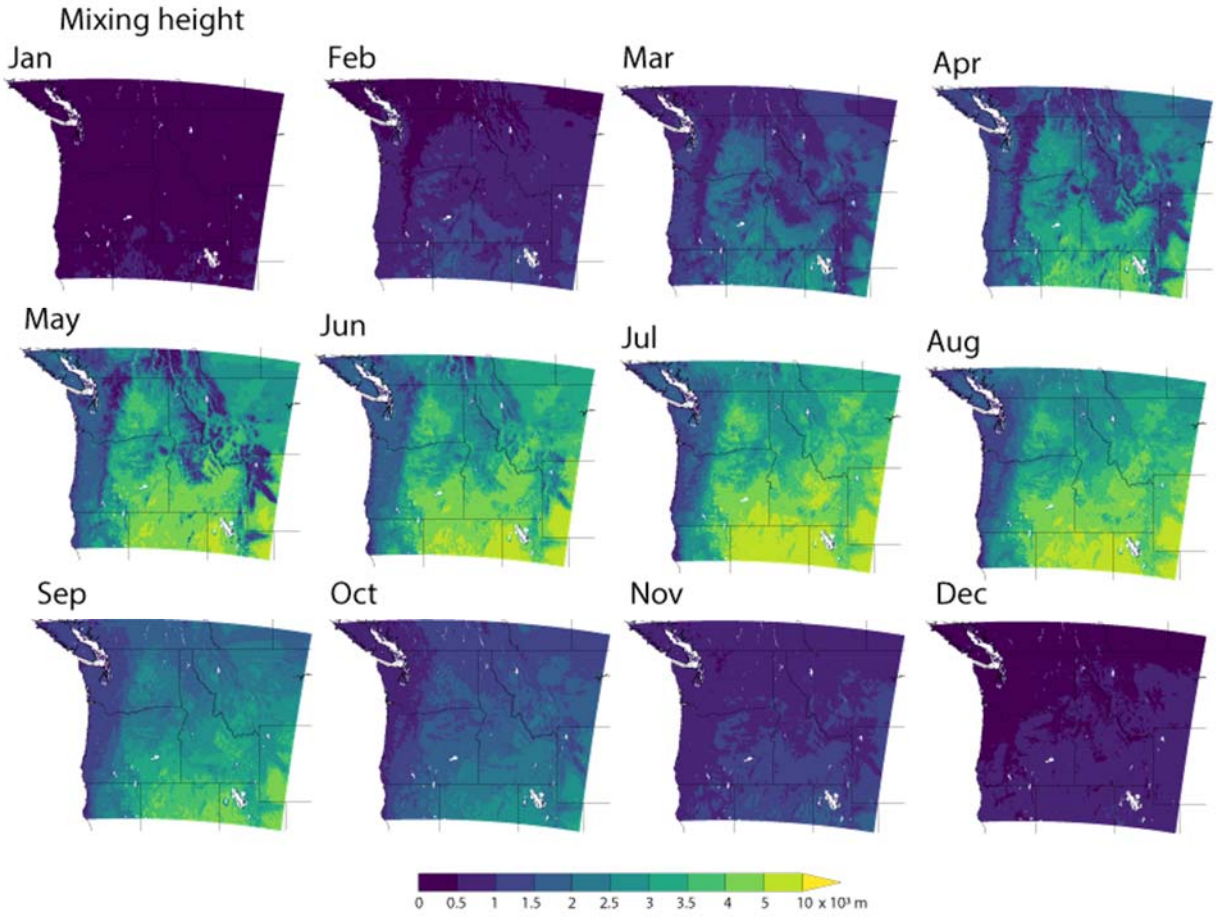

Figure 2. Climatological monthly mean daytime (10am – 2pm local) mixing height based on June 2009 – December 2018 4km University of Washington Weather and Forecasting Model (WRF) data

The transport wind monthly climatology exhibits character broadly comparable to the mixing height climatology. For example, transport winds are lower over most of the region in the cool season months (November through February) than in the spring and summer (Fig. 3). Some exceptions to this type of seasonality, however, can be seen along the eastern flanks of the Rocky Mountains in Montana and Wyoming and crest of the Washington Cascades. Evidently, lower level wind speed enhancements in these areas during the cooler months (e.g. February) cause cool-season transport wind amplitudes above summertime levels.

The transport wind depence on mixing height clearly shapes its regional-mean seasonality. Wind speeds tend to increase with height above ground in all. Summertime mixing heights are generally higher than in winter. Thus, the seasonal change in height over which transport wind is calculated largely counters the effect of wind speeds at any given height being stronger, on average, in winter than summer.

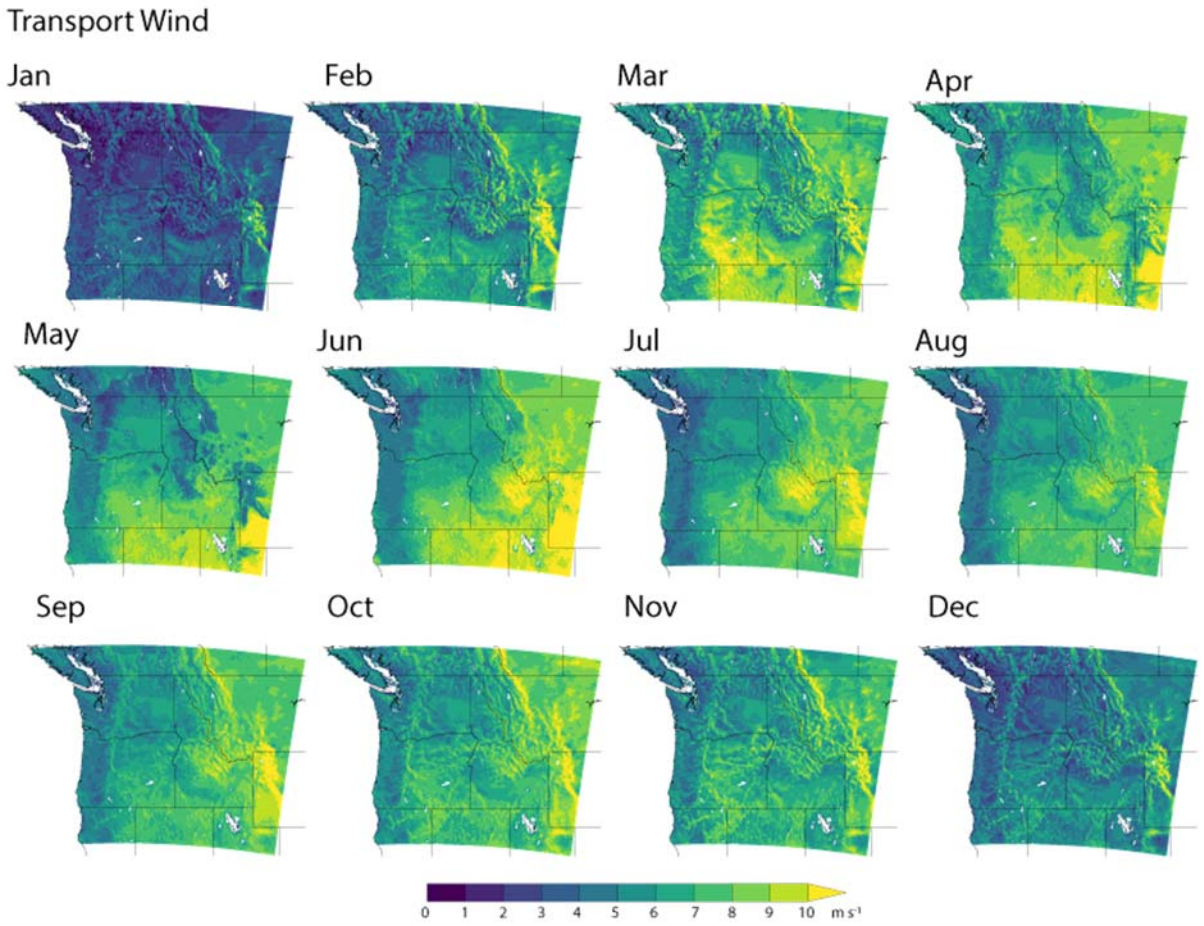

Figure 3. Climatological monthly mean daytime (10am – 2pm local) transport wind based on June 2009 – December 2018 4km University of Washington Weather and Forecasting Model (WRF) data

This situation is illustrated for a grid point within the Okanogan-Wenatchee National Forest in Figure 4, wherein June and December averaged wind speed profiles and mixing heights are plotted. June averaged mixing heights are high enough at ~1600m that the speed reduction caused by turbulent friction in the near-surface layer (< 100 m) has a much smaller impact on the transport wind than in December, when the mean mixing height is about a tenth as large. Sub-monthly correlation between height and wind speed also contributes differently to the monthly mean transport wind in December and June (Fig. 5). Particularly, highest heights tend to occur during moderate winds in June, whereas December exhibits a tendency for strongest winds and highest heights to co-occur (suggesting near-ground mechanical turbulence plays more of a role in deepening the mixed layer in winter). That the highest ventilation index values in June occur during more moderate wind speeds, and thus conditions more conducive to controlled fire management, suggests that such times may be ideally suited for ‘natural prescribed burns’ (as discussed below).

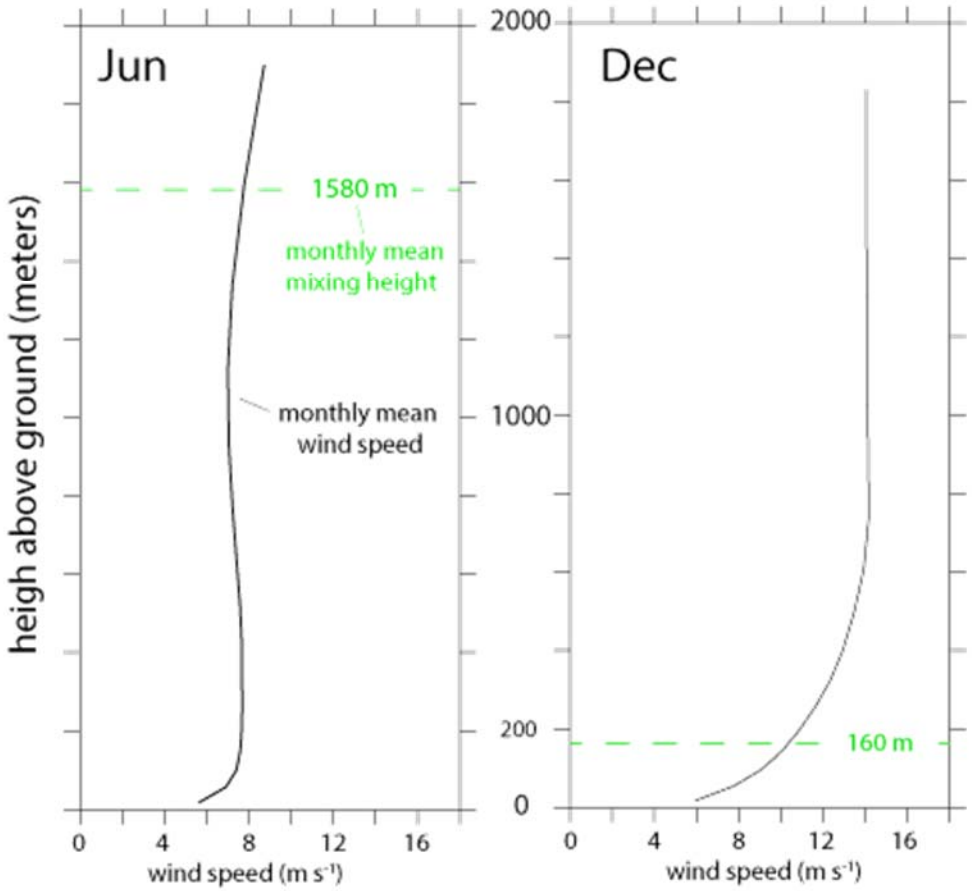

Figure 4. June and December climatological average wind speed profiles at a grid point within the Okanogan-Wenatchee National Forest of Washington. Climatological average mixing heights are denoted by the green dashed lines, with the December value still in the slower near-surface layer.

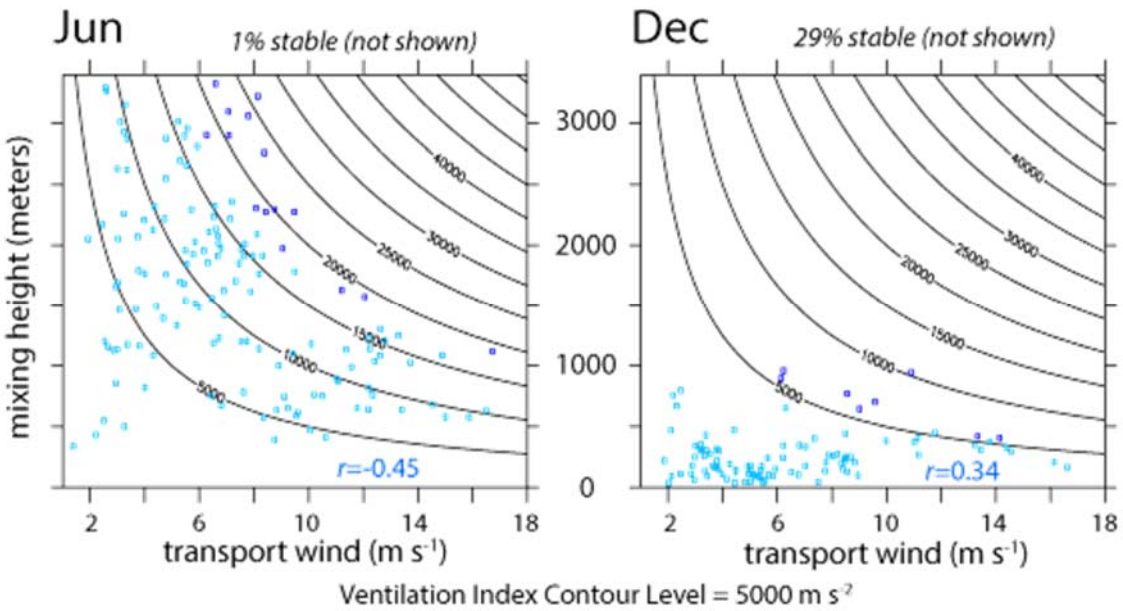

Figure 5. Day-time averaged transport wind versus mixing height during June and December. The correlation between these two variables changes sign moving from June (r = -0.45) to December (r = 0.34).

Monthly climatological day-time average ventilation index exhibits dramatic gradients across space and time, with summertime amplitudes at or above thresholds typically considered sufficient (good) for dispersing smoke from prescribed burning (e.g. > 8000 m2/s). Summertime western Washington and Oregon values lie in typical 'fair' to 'moderate' ranges (4000 – 8000 m2/s). These seasonally-high heights fall-off moving to spring and fall, with especially sharp declines between March and February and September and October (Fig. 6). Washington prescribed burning mainly takes place in the spring and fall with an overall maximum in October and secondary maximum in April-May (Fig 7). The Northwest burn seasons coincide with seasonal peaks in the rate of change of atmospheric dispersion.

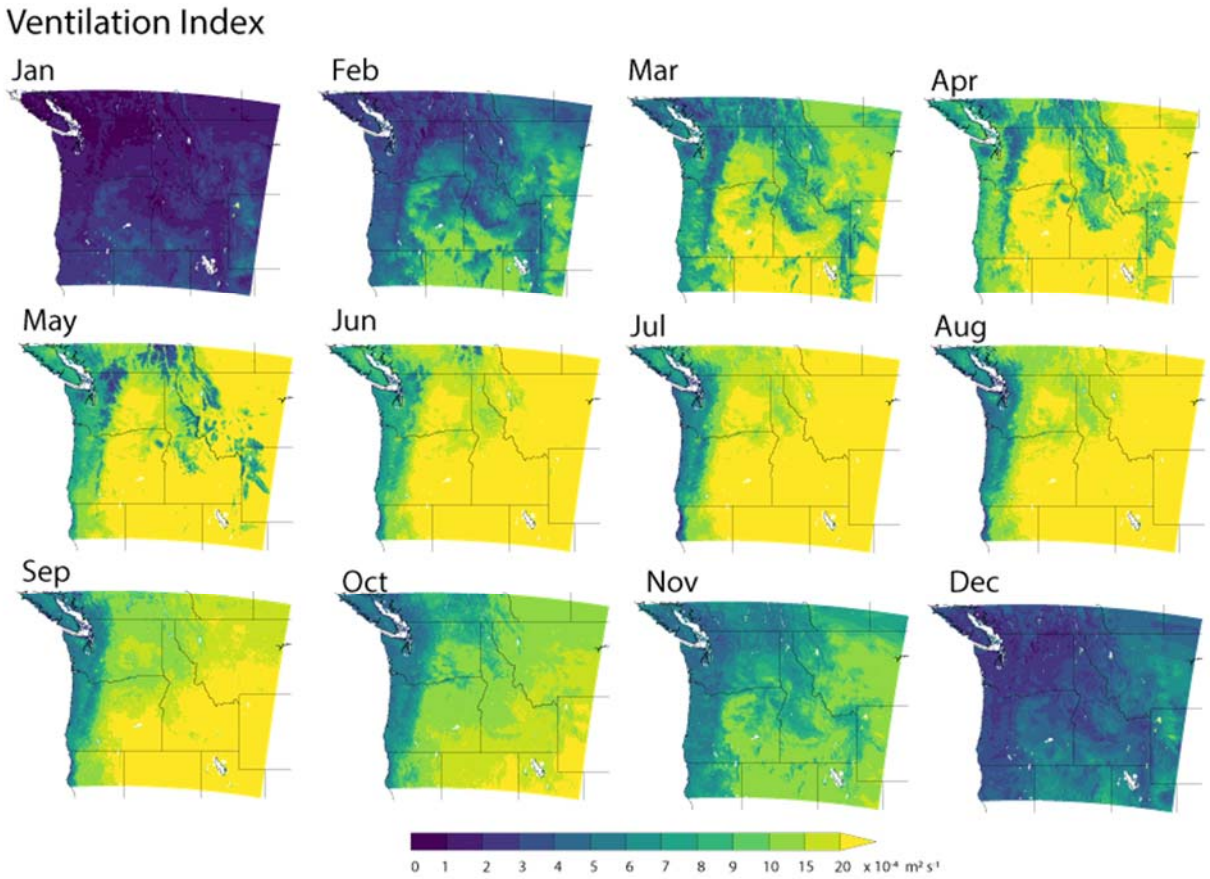

Figure 6. Climatological monthly mean daytime (10am – 2pm local) ventilation index based on June 2009 – December 2018 4km University of Washington Weather and Forecasting Model (WRF) data.

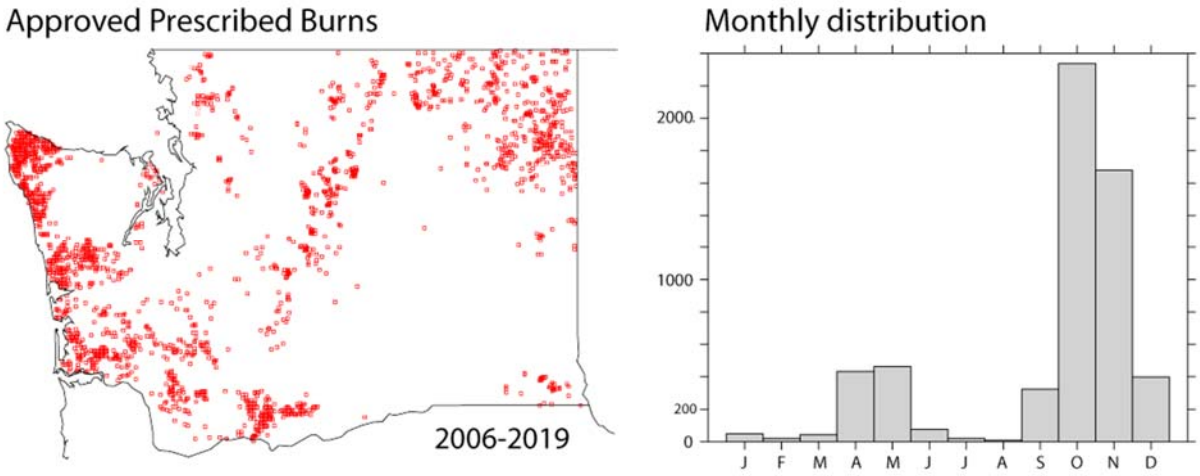

Figure 7. Washington prescribed burn spatial and monthly distribution.

Hourly climatology

Maps of climatological mean hourly mixing height averaged over spring, summer and fall is offered in Figure 7. Highest heights at each hour are generally seen in the summer. And during summer, heights >1200 m appear earlier in the morning (9am PDT), and last longer into the evening (> 5 pm PDT) than in the spring or fall. Comparison of spring and fall mixing heights reveals that the spring is preferable to the fall from a smoke dispersion perspective (higher mixing heights), with the exception of area of peak elevation (e.g. crest of the Cascade Mountains of Oregon and Washington) where, presumably, stronger autumn winds help spur mixing.

Hourly climatological transport wind increases during the morning hours (Fig. 8) with timing similar to mixing height (e.g. approx. 3-fold increase from 7am to 11am PDT; c.f. Fig. 7). Seasonal variability of transport wind is more subdued than mixing height, however. For example, 1 pm mixing height over eastern Oregon and Washington varies by a factor of ~2 (Fig. 7) with change in season (summer to spring or fall), which is nearly an order of magnitude larger than the ~25% change seen across seasons in transport wind (Fig. 8).

Taking >8000 m2/s as the rule-of-thumb for good, and > ~6500 m2/s for conditionally-good prescribed burn smoke dispersion conditions (as in Utah and Montana) we see that adequate or near-adequate dispersion is reached over about half of eastern Oregon and Washington by 9 am PDT in the summer (Fig. 9) and all of eastern Oregon and Washington by 11 PDT. Good dispersion is then seen over the majority of the inland Northwest until at least 5 pm PDT during summer, while ventilation index conditions over western Washington and Oregon remain mostly at or below 6500 m2/s. Good ventilation is also seen mid-day over the interior Northwest during spring and fall (Fig. 9), however, high ventilation index values are reached later in the morning and terminate sooner in the afternoon compared to summer at most interior locations. The mean seasonal cycle of ventilation over southwestern Oregon is different in character than the interior, with a maximum in spring.

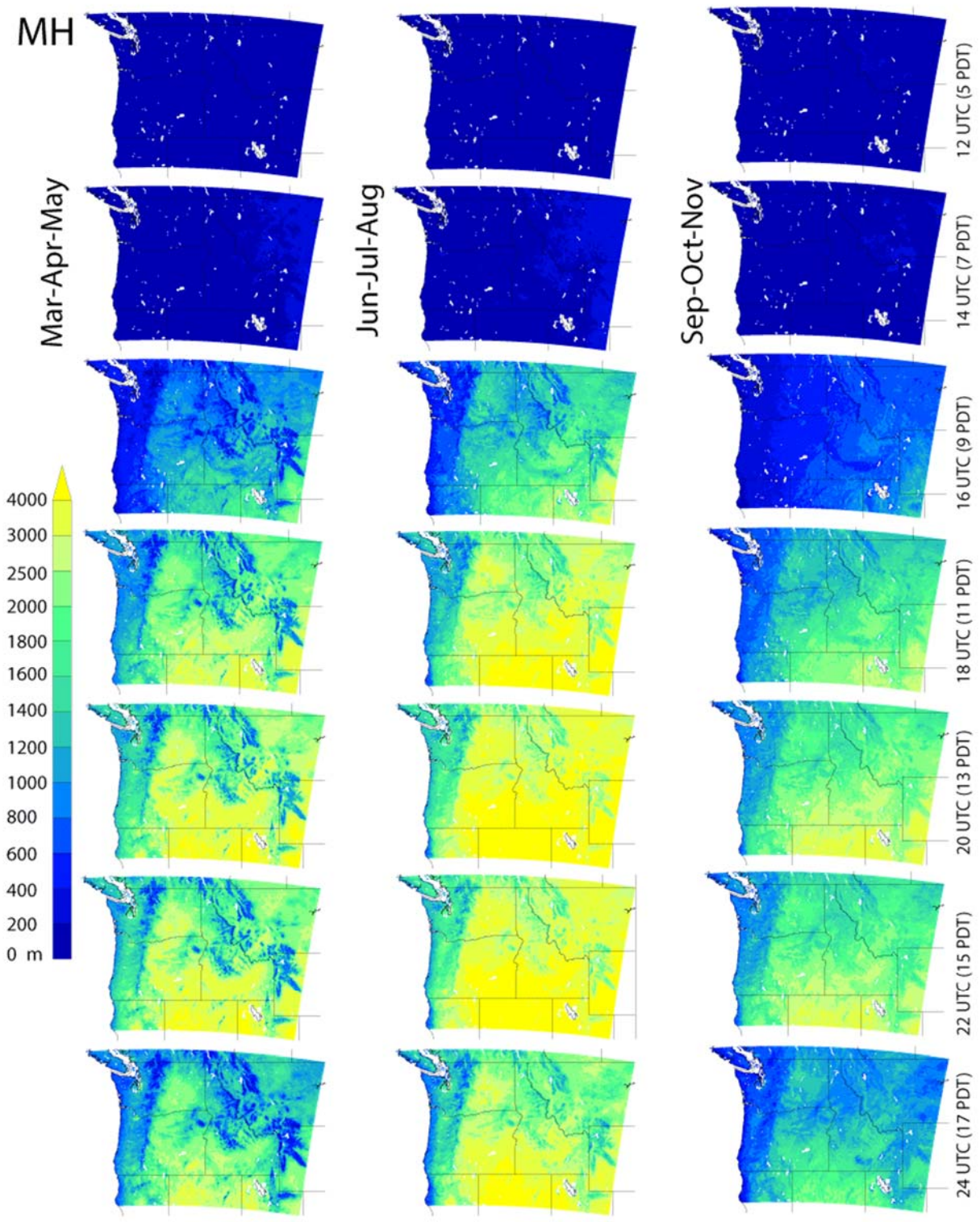

Figure 8. Hourly climatological mixing height, for selected 5am to 5pm PDT hours, averaged over spring (Mar-Apr-May), summer (Jun-Jul-Aug) and fall (Sep-Oct-Nov).

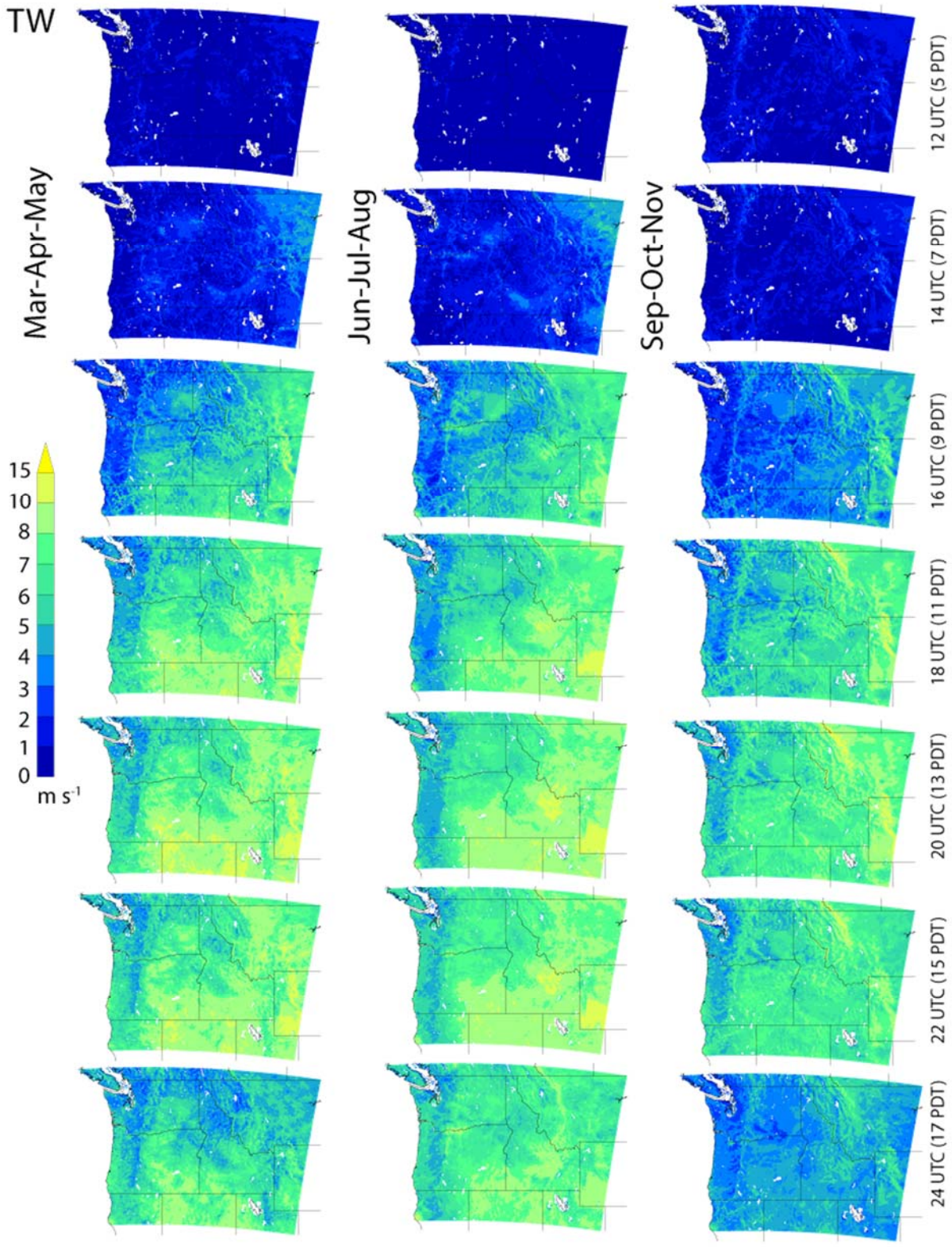

Figure 9. Hourly climatological transport wind, for selected 5am to 5pm PDT hours, averaged over spring (Mar-Apr-May), summer (Jun-Jul-Aug) and fall (Sep-Oct-Nov).

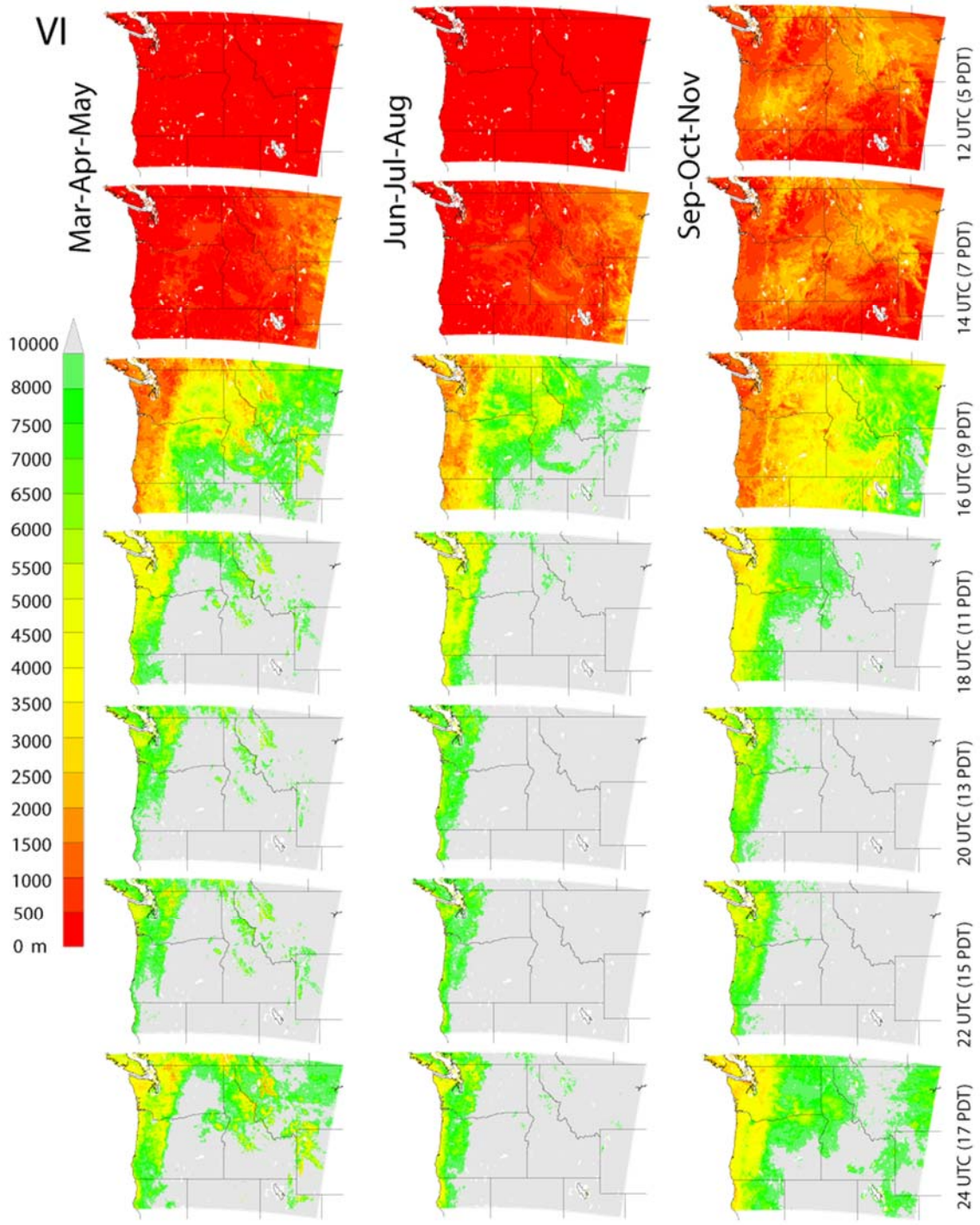

Figure 10. Hourly climatological mixing height, for selected 5am to 5pm PDT hours, averaged over spring (Mar-Apr-May), summer (Jun-Jul-Aug) and fall (Sep-Oct-Nov).

4. Parameter sensitivity.

Near-surface (10m) wind speed is substituted for transport wind speed when calculating 'ventilation index' by some Northwest States (e.g. Washington). This motivates examination of the relationship between these two variables. Focus here will be on the spring through fall, when the majority of prescribed burns take place, or could take place (in summer) in the form of naturally ignited, yet carefully controlled burns.

Regionally and monthly climatological average transport wind ranges from 6.5 to 7.6 m/s moving from spring to fall, with a mean of 7.0 m/s (Fig. 11, upper panel). Meanwhile, 10m transport wind varies from 3.1 to 4.4 m/s, with spring-to-fall mean of 3.7 m/s. The ratio of 10-m wind to transport wind speed is near minimum in summer at ~ 0.5 and reaches ~0.6 in early spring and late fall, in a regionally averaged sense (Fig. 11, lower panel).

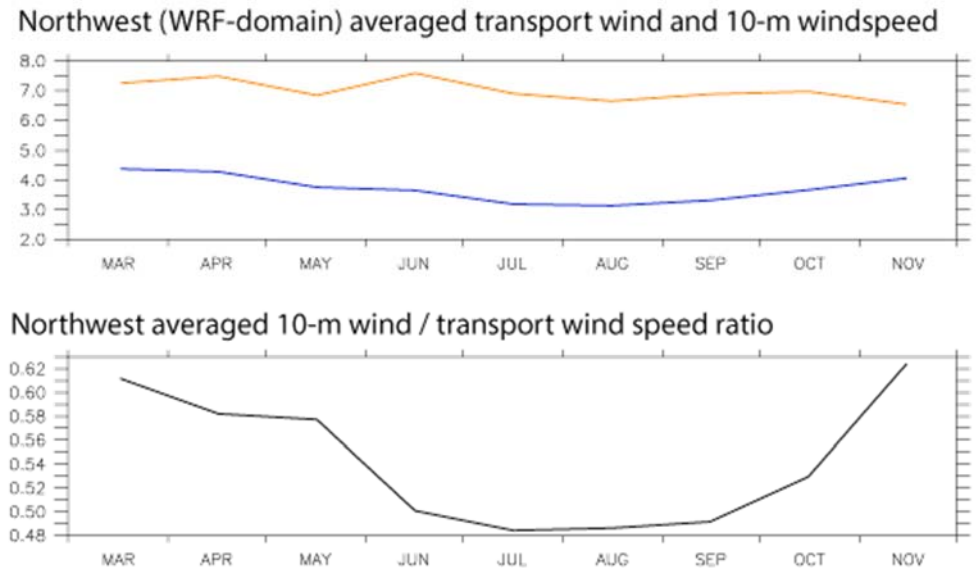

Figure 11. Upper: Regionally averaged transport wind (red) and 10-m windspeed (blue). Lower: Ratio of 10-m wind to transport wind speed in a region-averaged sense.

This ratio, however, exhibits large spatial variability. Particularly low (~0.25) values are seen during summer in southeastern Oregon and the higher elevations of central Idaho and southwestern Montana (Fig. 11). Values approach unity, on the other hand, are seen in spring along the higher elevations of the Cascade Mountains in Washington. Southwestern Oregon exhibits unique character in that (unlike most locations) higher ratios are seen in summer than in fall or spring.

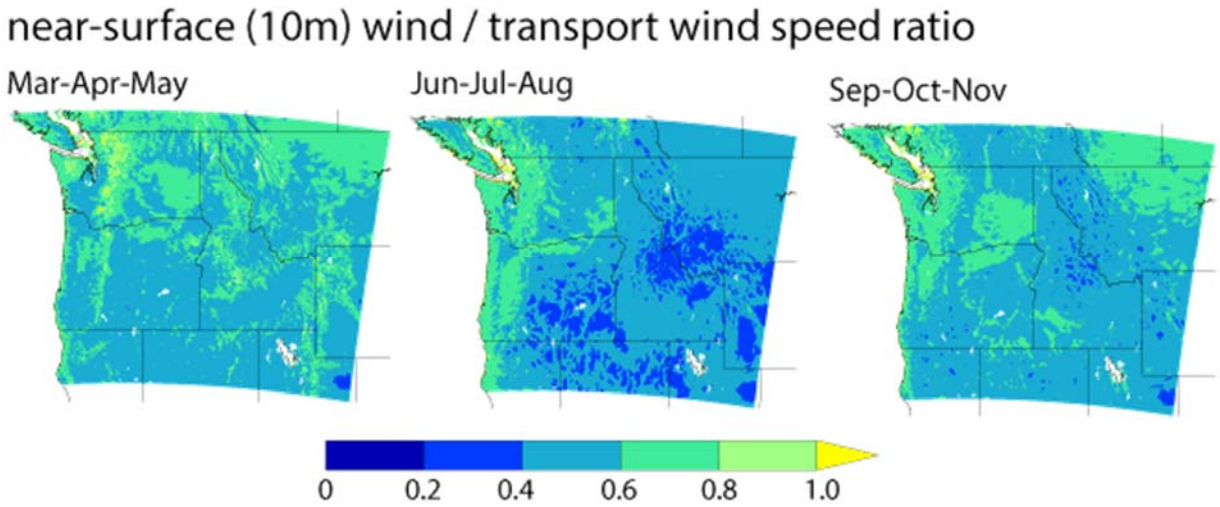

Figure 11. Ratio of 10m wind speed to transport wind speed, calculated based on daytime-averaged WRF data, averaged over spring (Mar-May), summer (Jun-Aug) and fall (Sep-Nov), period 2009-2018.

Thus, in a region-averaged sense, the main effect of substituting near-surface for transport wind in the ventilation index calculation is to lower magnitudes by about a factor of two. Over most locations, this substitution also acts to partially flatten-out the mean seasonal cycle contributed by mixing height, which is highest in summer. Particular locations such as southwestern Oregon, however, exhibit seasonality in wind ratio that is different in character from the regional mean behavior. Thus, a spatially varying set of effects are evident by comparing seasonal maps of 10m-wind-based ventilation index (VI_{10}; Fig. 12) with the results of the traditional calculation methods (Fig 10).

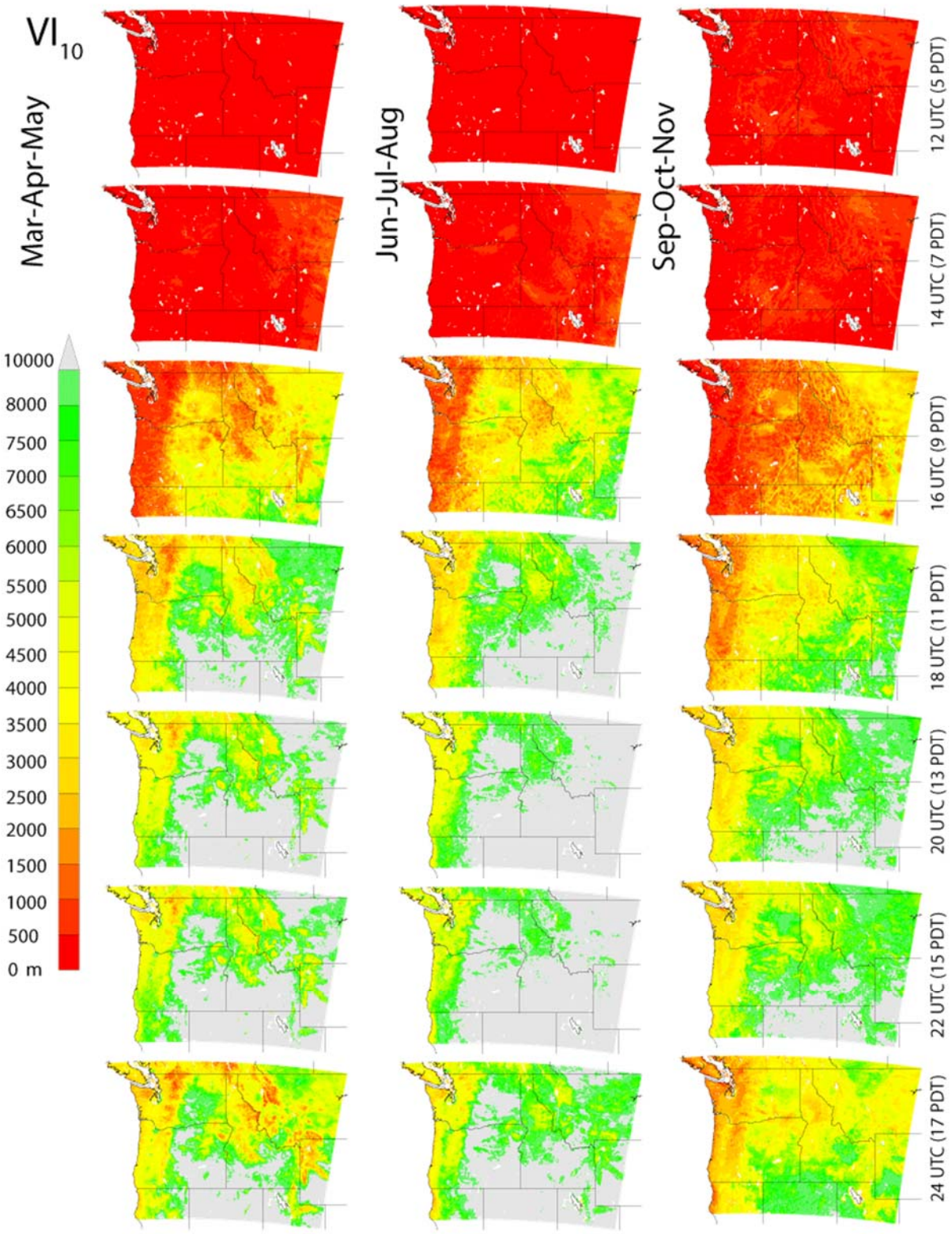

Figure 12. Same as Fig. 10, except using 10m wind speed rather than transport wind to calculate ventilation index.

5. Characterizing variability.

Daytime averaged ventilation index data at 4km horizontal resolution was re-gridded to 25km spacing to facilitate an empirical orthogonal function (EOF) analysis; that is, the statistical separation of its temporal and spatial variability into distinct (in the linear statistical sense) modes of variability. The first spatial mode in conjunction with the first temporal mode explains 67% of the total daily variance contained in the full (all season) 2009-2018 data set. Peaks in the first spatial mode are seen along the higher elevation plateaus in the southern part of the study region, including the upper Snake River Plain of Idaho, the great basin regions of northern Nevada and southeastern Oregon, and the Greater Green River Basin of southwestern Wyoming. Secondary maxima are located over the Columbia Plateau and plains of north-central Montana. Amplitudes are smallest along western Washington, western Oregon and near Utah's Great Salt Lake (Fig. 13).

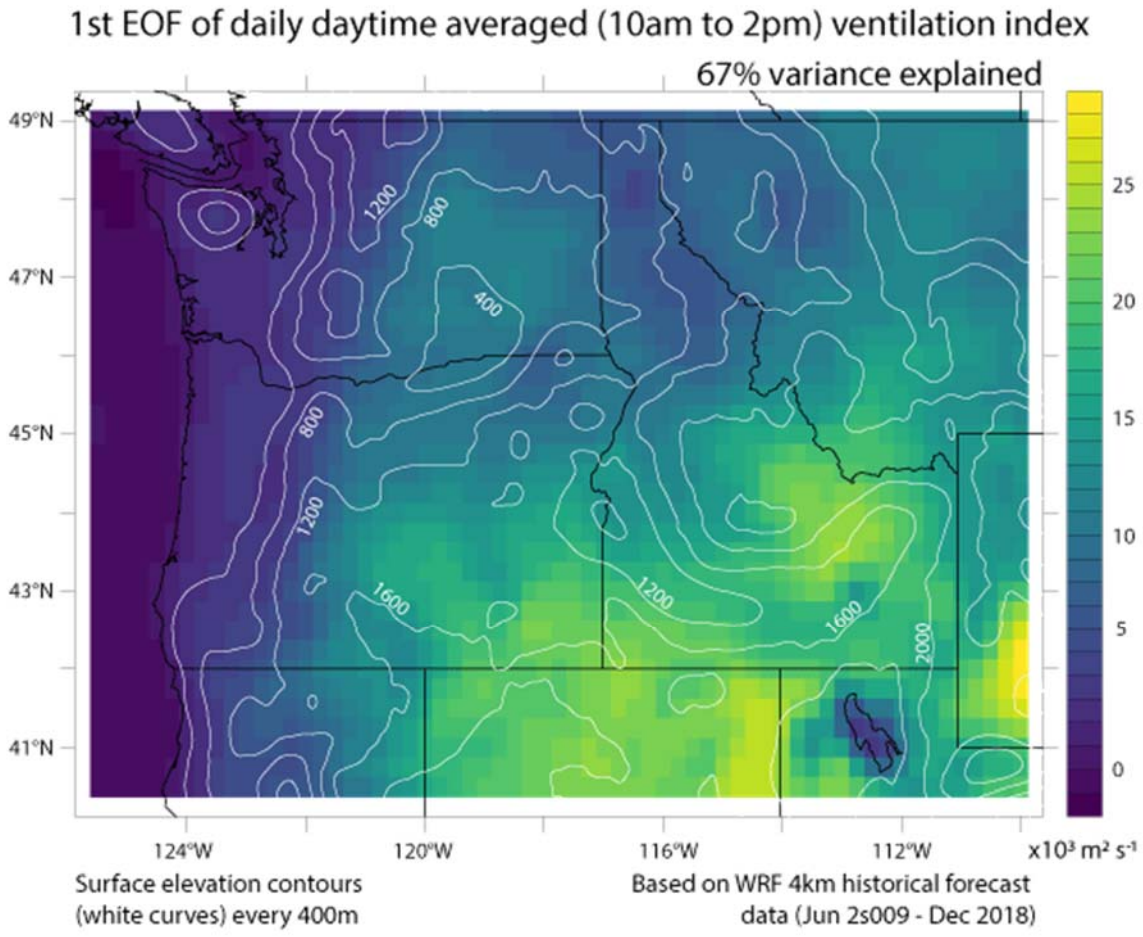

Figure 13. 1st empirical orthogonal function of daytime ventilation index (shading), with smoothed surface elevation contours.

The time series associated with the first spatial mode is shown in Fig. 14 (period 2013-2018.) It contains a strong seasonal cycle with minima in winter, maxima in later spring and summer. Variability is enhanced in the warm seasons. Experimentation reveals that even after the mean seasonal cycle of ventilation index is removed from each grid point, this mode retains its spatial structure and still explains over half of the (non-seasonal) variability. The other modes each account for less than 10% of ventilation index variability.

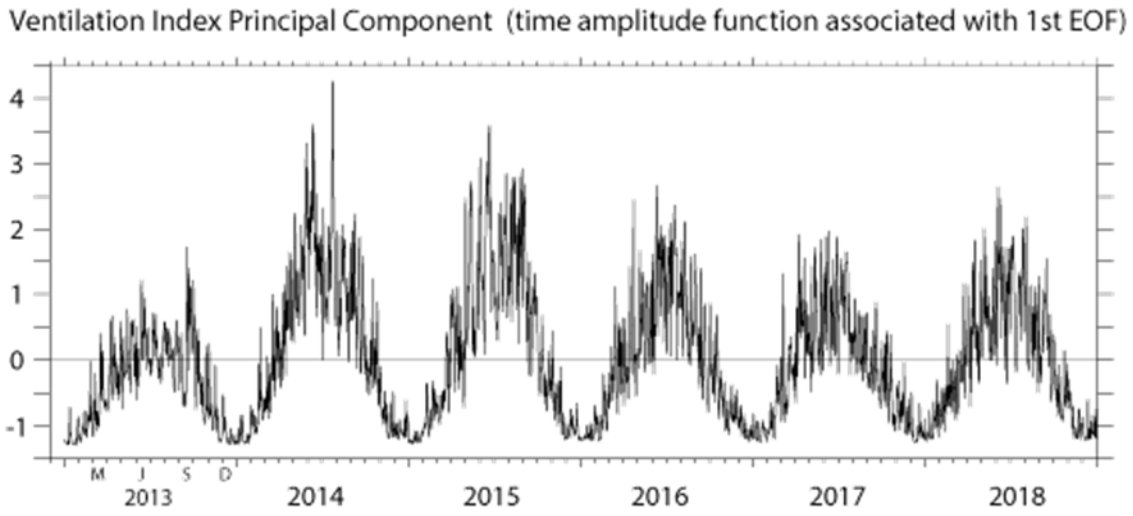

Figure 14. Principal component (1st EOF) of Northwest ventilation index variability.

Restricting the area considered in the EOF calculation to that around Washington and Oregon does little to alter the spatial pattern of the 1st mode, which continues to exhibit maxima in southeastern Oregon and the Washington Columbia Basin (Fig. 15, left). The principal component associated with the 1st spatial mode over Washington and Oregon is also very highly correlated with the Northwest regional result, especially in the cooler seasons (Fig. 15; right panel).

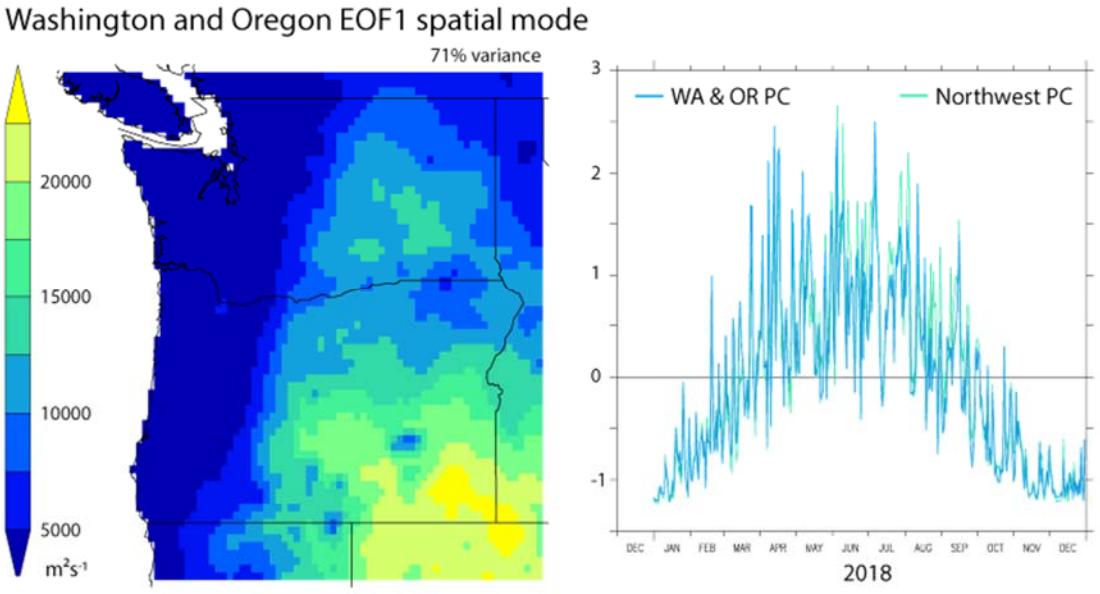

Figure 15. Left: 1st EOF of daytime ventilation index over Washington and Oregon. Right: Time series associated with the 1st Washington and Oregon mode (blue curve) overlaid with the Northwest regional result (green curve) for 2018.

The 1st EOF modes of mixing height and transport wind are shown in Figure 16, along with their principal components. Comparison of EOF1 of mixing height and transport wind reveals broad similarities in spatial structure with maxima generally located in the inland and southern parts of the study region and minima along the Pacific coast. This rough spatial similarity can be understood in large part by considering the way the transport wind calculation dependends on mixing height (e.g., higher heights causing the vertical average upon which transport wind is based to include stronger winds aloft). Thus, EOF1 of transport wind and mixing height are highly correlated with one another in terms of spatial structure (r_{space} = 0.90), and highly correlated with EOF1 of ventilation index (spatial correlation with ventilation index EOF1 = 0.90 and 0.95 for transport wind and mixing height, respectively).

Transport wind and mixing height principal components are much less well correlated with one another in time (r = 0.3; see Fig. 17's lower panel) than space. Mixing height principal component variability is dominated by a strong seasonal cycle, accounting for 60% of its temporal variability, and highly correlated (r= 0.87) with the principal component of ventilation index. Based on the traditional correlation-squared estimate for 'variance explained', approximately 75% of the temporal variability associated with the 1st EOF of ventilation index can be explained by EOF1 of mixing height. Transport wind temporal variability is different in character than mixing height (r= 0.37), with peaks of similar amplitude occurring from about February to October and minima during the winter. Transport wind is less well correlated with ventilation index variability (principal component correlation = 0.46) than mixing height. Transport wind variability, however, does effectively expand the number of months over which peaks in ventilation occur (c.f. Fig. 16, lower panel).

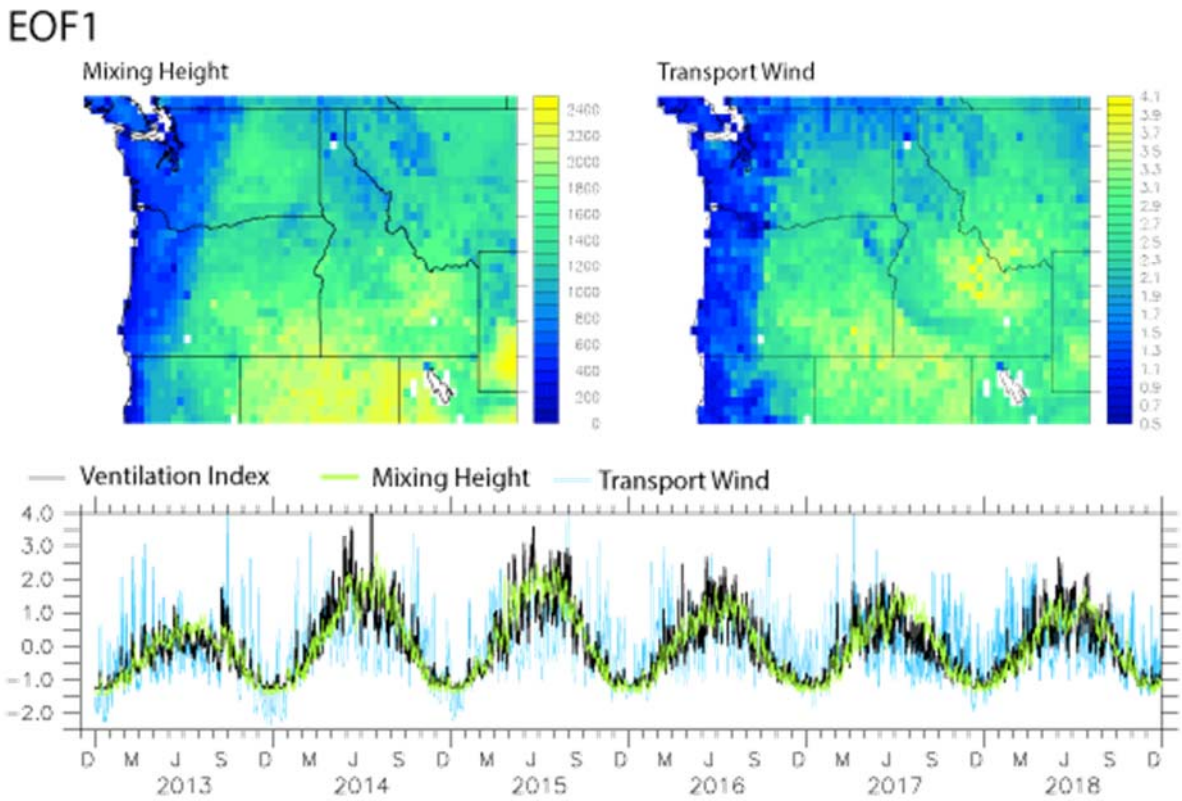

Figure 16. Upper left: First spatial mode of daytime mixing height variability based on empirical orthogonal function (EOF) analysis. Units = m. Upper right: Same as upper left, except for transport wind (units = m/s). Lower panel: Time functions associated with the 1st EOF mode (principal component) of ventilation index, mixing height and transport wind.

The EOF analysis above suggests mixing height variability to be the dominant driver of ventilation index conditions over especially the higher elevation plateaus of the southern half of the study region. But how well does this assessment hold over forested mountain flanks targeted for prescribed burning? To gauge this in the case of the North Cascades, ventilation index was averaged over the eastern Cascade Mountain flanks of Washington and lower British Columbia and the effects of mixing height and transport wind variability alternately removed by substituting their time-means for their original daytime averages (at each grid point prior to spatial averaging). Results confirm what is suggested by the EOF analysis, that most of the temporal ventilation index variability over this area, including its strong seasonal cycle, is contributed mainly by mixing height variability, with transport wind playing a secondary role that contributes some additional shorter timescale (a week or two) peaks in the warmer seasons (spring through fall).

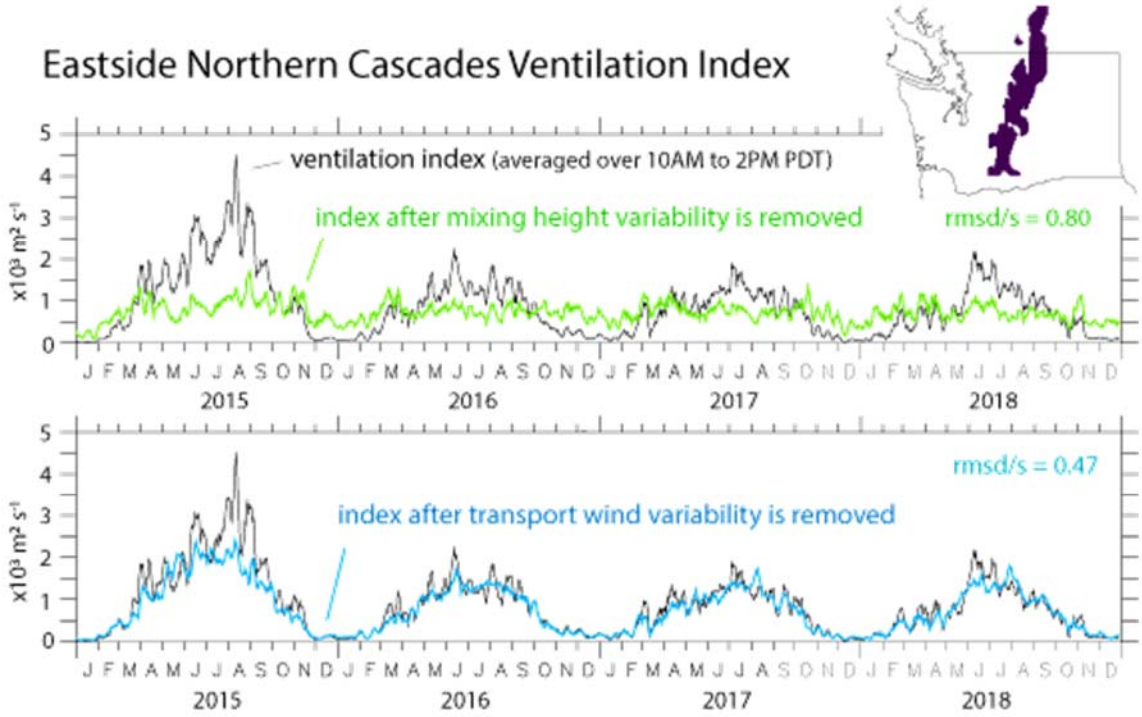

Figure 17. Ventilation index (black curve repeated in each panel) shown overlaid with the effect of removing its constituent mixing height (lower panel) and transport wind (upper panel) variability by replacing these variables with their respective time-averages. The ratio of the root-mean-square difference (rmsd) between the original and modified ventilation index time series and the original standard deviation (i.e. signal-strength) is listed in each panel. By this measure the 'signal-to-noise' ratio caused by removing a given component's variability is approx. 2 (usefully large) in the transport wind case and nearly 1 (signal hardly recognizable) in the mixing height case. Mixing height is clearly the dominant driver of the ventilation index variability over the eastern flank of the Cascade Mountains shown in the map inset to the upper right.

6. Summary and next steps.

The ventilation index, traditionally calculated as mixing height times transport wind, provides a fundamentally important measure of the atmosphere's capacity to disperse smoke. Ventilation forecasts are critical to operational decisions about when prescribed burning is or is not allowed from the smoke (i.e. breathable air quality) perspective. The core atmospheric variables upon which mixing height and transport wind depend, such as surface and vertical profiles of temperature, pressure, humidity, and wind, have been forecasted by the Northwest Regional Modeling Consortium based on 4km horizontal resolution Weather Research and Forecasting (WRF) model runs conducted at the University of Washington for the last ~10 years. The calculation of hourly mixing height, transport wind and ventilation index from these historical weather forecasts has allowed the monthly seasonal cycle of these fire-related weather forecast variables to be documented over this period and the 4km-WRF domain, which includes all of Oregon and Washington (USDA Forest Service Region 6) and extends south to Northern California and east to the Great Plains of Montana and northeastern Utah. This climatology

serves to update and compliment previous efforts to estimate the mean seasonal cycle of ventilation based on available (sparse) observational measurements (e.g. Ferguson et al. 2003; mixing height based on 4 stations spread over all of Washington and Oregon).

The curation of this information also offers useful basis for several future projects that are anticipated to be of interest to the Forest Service and other agencies and managers involved in prescribed burning or its governance. These include using this data base to:

- Calculate the historical weather windows for prescribed burning and **quantify the effects of proposed prescribed burn policy changes**

- Build an **online tool** that burners can use to **calculate probability** of **burn** weather **windows**

- Study the **linkages** between the weather and fuel moisture parameters controlling **smoke dispersion**, **fire behavior** and regional atmospheric **circulation patterns**.

The results described herein provide building blocks that will help support these efforts. For example, because Washington prefers using 10m winds rather than transport winds when calculating ventilation index, the quantification of their relationship (fixed height to transport wind ratio) provided in Section 4 enables comparison of proposed Washington smoke management policy changes with the practices of other Northwest States. Further, the identification of the dominant mode of ventilation variability over the inland Northwest (Section 5) provides a useful focus for future examination of its links to fire behavior weather and fuel parameters.

Wildfire activity over Washington and Oregon in 2019 was much less intense than in 2017 and 2018. This meant that crews that would have been fully involved in suppression efforts in years like 2017 or 2018 would have been available to work toward other management goals in 2019. This motivated a recent request for scientific information from Forest Service Region 6 (serving Washington and Oregon). As mentioned above, in years like 2019, if naturally ignited fires can be managed for fuel treatment and ecological benefits, rather than being extinguished immediately, this could greatly expand the acres burned over the Northwest and thereby restore fire resiliency to regional forests in a cost-effective manner. Public acceptance of a change in the way wildfire is managed – essentially willingness to put up with some amount of smoke - will be needed to do this. If it can be shown that ventilation conditions associated naturally ignited wildfires are preferable to those typically associated with prescribed burns, this would provide useful information to the ongoing discussion about how to come up with the best overall fire and smoke management policy. The documentation of ventilation index behavior over the Northwest provided herein provides fertile ground for such study.

7. References

Chiodi, A.M., N.K. Larkin, J.M. Varner, and J.K. Hiers (2019): Sensitivity of prescribed burn weather windows to atmospheric dispersion parameters over southeastern USA. Int. J. Wildland Fire, doi: 10.1071/WF18209

Chiodi, A.M., N.K. Larkin and J.M. Varner (2018) An analysis of Southeastern US prescribed burn weather windows: seasonal variability and El Niño associations *International Journal of Wildland Fire* , 27, 176-189, doi: 10.1071/WF17132.

Fearon MG, Brown TJ, Curcio GM (2015) Establishing a national standard method for operational mixing height determination. *Journal of Operational Meteorology* **3**, 172–189. doi:10.15191/NWAJOM. 2015.0315

Ferguson, S.A., S.J. McKay, D.E. Nagel, T. Piepho, M. L. Rorig, C. Anderson and L. Kellogg. (2003). Assessing Values of Air Quality and Visibility at Risk from Wildland Fires. USDA Forest Service, Pacific Northwest Research Station Research Paper PNW-RP-550.

Goodrick SL, Achtemeier GL, Larkin NK, Liu Y, Strand TM (2013) Modelling smoke transport from wildland fires: a review. *International Journal of Wildland Fire* **22**, 83–94. doi:10.1071/WF11116

Haines TK, Busby RL, Cleaves DA (2001) Prescribed burning in the South: trends, purpose and barriers. *Southern Journal of Applied Forestry* **25**, 149–153.

Hall, F.C. 1976. Fire and vegetation in the Blue Mountains – implications for land managers. Tall Timbers Fire Ecology Conference Proceedings 15: 155-170

Hardy, C., R.D. Ottmar, J. Peterson, J. Core, comps., eds. 2001. Smoke management guide for prescribed and wildland fire: 20001 edition. PMS 420-2. Boise, ID: National Wildfire Coordinating Group. 226 p.

Holzworth GC (1967) Mixing depths, wind speeds and air pollution potential for selected locations in the United States. *Journal of Applied Meteorology* **6**, 1039–1044. doi:10.1175/1520-0450(1967)006,1039: MDWSAA.2.0.CO;2

Kobziar, LN, D. Goodwin, L. Taylor, AC Watts (2015) Perspectives on trends, effectiveness and impediments to prescribed burning in the southern U.S. Forests 6, 561-580.

Martin, R. E., & Dell, J. D. (1978). Planning for prescribed burning in the inland northwest. *Gen. Tech. Rep. PNW-GTR-076. Portland, OR: US Department of Agriculture, Forest Service, Pacific Northwest Research Station: 1-67*, *76*.

Mass, C. F., et al. (2003), Regional environmental prediction over the Pacific Northwest, *Bull. Am. Meteorol. Soc.*, 84(10), 1353– 1366.

Prichard, S.; Larkin, N.S.; Ottmar, R.; French, N.H.; Baker, K.; Brown, T.; Clements, C.; Dickinson, M.; Hudak, A.; Kochanski, A.; Linn, R.; Liu, Y.; Potter, B.; Mell, W.; Tanzer, D.; Urbanski, S.; Watts, A. The Fire and Smoke Model Evaluation Experiment—A Plan for Integrated, Large Fire–Atmosphere Field Campaigns. *Atmosphere* **2019**, *10*, 66.

Seibert P, Beyrich F, Gryning S-E, Joffre S, Rasmussen A, Tercier P (2000) Review and intercomparison of operational methods for the determination of the mixing height. *Atmospheric Environment* **34**, 1001–1027. doi:10.1016/S1352-2310(99)00349-0

Stull RB (1988) 'An introduction to boundary layer meteorology.' (Kluwer Academic Publishers: Boston, MA, USA)

Stull RB (1991) Static stability – an update. *Bulletin of the American Meteorological Society* **72**, 1521–1529. doi:10.1175/1520-0477(1991) 072,1521:SSU.2.0.CO;2